Study on high pressure design of contra-rotating small hydroturbine

IOP Conf. Series: Earth and Environmental Science **240** (2019) 042013 doi:10.1088/1755-1315/240/4/042013

Study on high pressure design of contra-rotating small hydroturbine

Takuji Hosotani[1], Toru Shigemitsu[2], Yuki Kawaguchi[1] and Tomofumi Ikebuchi[1]

[1] Graduate School of Advanced Technology and Science,
Tokushima University, 2-1 Minamijyosanjima-cho, Tokushima, 770-8506, JAPAN
[2] Graduate School of Technology, Industrial and Social Sciences,
Tokushima University, 2-1 Minamijyosanjima-cho, Tokushima, 770-8506, JAPAN

E-mail : hosotani.takuji@tokushima-u.ac.jp

Abstract. It is requested that the hydroturbine is small size and high performance. Therefore, we adopted contra-rotating rotors, which can be expected to achieve small size and high performance. However, when the rotors become smaller, the output power of conventional contra-rotating rotors, which is composed of axial flow rotors, is very low. In order to achieve small size and high output power, we propose new type contra-rotating rotors, which is composed of a hybrid rotor and a centrifugal rotor. In this research, we investigate performance of the new type contra-rotating small hydroturbine model by the numerical analysis. We report on the influence of deflection angle on the performance and internal flow condition.

1. Introduction

There is a strong demand to change energy resources of fossil fuels into renewable energy such as hydropower, wind power, solar energy and so on. Small hydropower generation is alternative energy, and there is a significant potential for small hydroturbine. Small hydropower facilities that generate about 100[kW]-1000[kW] have spread widely. However, it causes environmental destructions by foundation construction and set up of a draft tube. On the other hand, there are a lot of places that can generate about 100[W]-1[kW] (pico-hydropower) in agricultural water and a small stream. Small hydropower installations are expected to have lower environmental impacts, and the spread of small hydropower installations which effectively use these small hydropower resource is important. Therefore, darrieus and gyro-type turbines, which were suitable for the design specification of low head in agricultural water and a small river, were investigated and the performance characteristics and the optimum design parameter were discussed [1,2]. Internal flow of a spiral water turbine with wide flow passage, which had small environmental impact, was investigated [3]. Further, a small-cross flow turbine used for a small stream as an environmentally friendly pico-hydroturbine and a savonius turbine with low cost were suggested, and its performance improvement were reported by installation of a shield plate and selecting the optimum position of it [4-6]. Efficiency of small hydroturbines is lower than that of large one. Then, there are demands for small hydroturbines to keep high performance. Therefore, we adopted contra-rotating rotors, which could be expected to achieve high performance. In this study, significant compact hydroturbine is named as a small hydroturbine. Final goal on this study is development of a small hydroturbine like electrical goods, which has high portability and makes an effective use of the unused small hydropower energy resource.

In a previous research, we selected some places in Tokushima Prefecture in Japan, where a small hydropower can be generated, and conducted field tests of head, flow rate, water quality and capacity utilization [7]. Then we investigated performance of the test model by the numerical analysis and a prospect to apply this small hydroturbine for pico-hydropower was confirmed [8]. After that, we designed and manufactured an experimental apparatus to verify the performance of it and investigated the internal flow condition by the numerical analysis results [9,10]. Because of the large loss between the front and rear rotors, we changed the geometry of the spoke from a cuboid to a cone. The performance and internal flow condition of this small hydroturbine was largely improved by this modification [11,12].

In this research, based on the previous research results, we considered improvement of present contra-rotating small hydroturbine to accomplish higher performance and smaller size. In order to achieve higher performance, a centrifugal impeller was adopted as a rear rotor instead of the axial flow impeller for the new contra-rotating small hydroturbine. As a first step of this research, we investigated performance of the new contra-rotating small hydroturbine by the numerical analysis. In the present paper, we report the influence of deflection angle which affect the performance of the hydroturbine. The relationship between the deflection angle and performance is clarified by the numerical analysis results and the suitable deflection angle for the new contra-rotating small hydroturbine is considered.

2. Rotor geometry and design parameter

The rotor and primary dimensions of the contra-rotating small hydroturbine are shown in Fig.1 and Table 1 respectively. The hydroturbine diameter is small as under 100[mm]. In order to achieve higher output power than conventional contra-rotating small hydroturbine(axial flow type), the centrifugal rotor was adopted as the rear rotor for this contra-rotating small hydroturbine. Also in contra-rotating type, it is desirable that the output powers of front and rear rotors are equal. Therefore, we proposed a hybrid rotor as the front rotor, which was composed of a axial flow rotor and a mixed flow rotor, to make the same high design head of the rear rotor using the centrifugal type. The fluid flows axially into the hydroturbine, and that is bent to inward direction of radius by the front rotor of hydroturbine. The fluid is bent to axial direction again by the rear rotor, and flows from the hydroturbine. By doing so, high output power can be expected because a centrifugal action can be used effectively.

Design flow rate and head were Q_d=8[*l*/s] and H_d=21.8[m] respectively based on output power, head, flow rate assumed in the pipe of agricultural water and the small-scale water-supply system. Design head of each front and rear rotor was the same as H_{df}=H_{dr}=10.9[m] and a rotational speed of each front and rear rotors of the hydroturbine were N_f=2500[min^{-1}] and N_r=4200[min^{-1}] respectively. The rotational speed of these rotors is high because the high head is achieved and the deflection angle of rotor doesn't become large extremely. Each design parameters were determined by the design output power, head, flow rate and rotational speed. In this study, blade number of each front and rear rotor should be a coprime; the front rotor Z_f=6 and rear rotor Z_r=7 in order to suppress blade rows interaction of the contra-rotating rotor. A guide vane was not set at the inlet of the front rotor because this hydroturbine was designed as compact as possible. The front rotor was designed that flow was axial direction at inlet side and that was inward direction of radius at outlet side. The rear rotor was designed that the inlet angle matched downstream of the front rotor and swirling flow did not remain downstream of the rear rotor at the design flow rate. When the rotors was designed based on these specifications, the shape of front rotor was like an inducer as shown in Fig.1(a). The rotor was the special shape, so we anticipated that the performance was very influenced by the deflection angle. Therefore, in order to investigate the influence of deflection angle θ, the meridian plane of each deflection angle model was the same shape, the inlet angles of rear rotor and the outlet angles of each front and rear rotors were changed from Table 1.

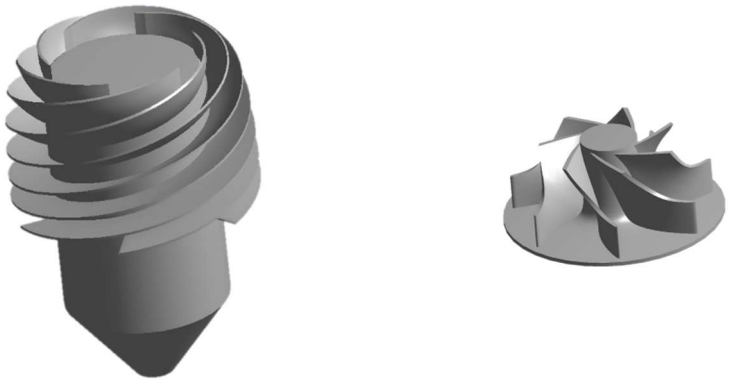

(a) Front rotor (b) Rear rotor

Fig.1 Overviews of hydroturbine rotor

Table 1 Primary dimensions of turbine rotors

			Hub	Tip
Front rotor (Hybrid type)	Diameter [mm]	Inlet	60	90
		Outlet	54	
	Blade width [mm]	Inlet	15	
		Outlet	8.7	
	Blade angle [deg]	Inlet	14.9	10.1
		Outlet	15.4	
	Blade number		6	
Rear rotor (Centrifugal type)	Diameter [mm]	Inlet	50	
		Outlet	14	34
	Blade width [mm]	Inlet	8.7	
		Outlet	10	
	Blade angle [deg]	Inlet	85.3	
		Outlet	71.6	51.1
	Blade number		7	

3. Numerical analysis method and condition

In the numerical analysis, the commercial software ANSYS-CFX 16.2 was used under the condition of 3D steady flow condition. Fluid was assumed to be incompressible and isothermal water and the equation of the mass flow conservation and Reynolds Averaged Navier-Stokes equation were solved by the finite volume method. The standard wall function was utilized near the wall and the Shear-Stress-Transport was used as the turbulence model. The numerical grids of the whole numerical regions used for the numerical analysis is shown in Fig.2. A numerical model was designed assuming the test section of the experimental apparatus in future works. The numerical region has inlet pipe, outlet pipe and hydroturbine which is composed of the front and rear rotor. The lengths of each inlet and outlet pipe regions are $10D_f$ and $10D_r$ respectively. A tip clearance is c=1[mm]. Each front and rear rotor's shaft was modeled in the numerical analysis and rotated in the front and rear rotor's rotational direction respectively. The constant velocity perpendicular to the inlet boundary and the

constant pressure having only axial velocity were given as the boundary condition at the inlet and outlet respectively. The numerical grid points of each region were about 1.3 million for the inlet and outlet pipe region, about 6.9 million for the front rotor region and about 2.1 million for the rear rotor region respectively. The numerical analysis was performed at design flow rate point.

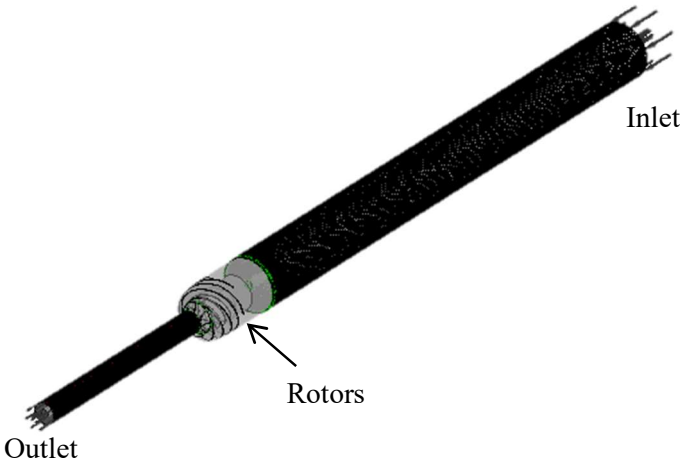

Fig.2 Numerical grids

4. Results and discussions

4.1. Performance curves

Performance curves of front rotor under the condition of different deflection angle obtained by the numerical analysis are shown in Fig.3. The flow rate is the design flow rate $1.0Q_d$. In this investigation, only the outlet angle of front rotor was changed. The rear rotor is not changed from Table 1, and the deflection angle of rear rotor is kept constant as θ_r=24[deg]. A horizontal axis is the deflection angle. First vertical axis is the turbine head and shaft power. Second vertical axis is the total pressure efficiency. The total pressure efficiency of front rotor η_f is calculated from the ratio of shaft power P_f to the input power of front rotor. The input power of front rotor was obtained by the multiplication of the flow rate Q and the mass flow averaged total pressure change of the front rotor, so the mass flow averaged total pressure change was obtained by the multiplication of the fluid density ρ, gravitational acceleration g and the turbine head H_f. The turbine head H_f was obtained from each interfaces of front rotor. Therefore, the total pressure efficiency of front rotor η_f was expressed in the following equation.

$$\eta_f = \frac{P_f}{\rho g Q H_f}$$

In the front rotor shown in Fig.3, the turbine head H_f and shaft power P_f increased according to the increase of deflection angle. The maximum efficiency $\eta_{f\,max}$=55.5[%] was obtained at θ_f=-4[deg]. The efficiency increased until θ_f=-4[deg], and decreased after θ_f=-4[deg], according to the increase of deflection angle.

Next, performance curves of rear rotor obtained by the numerical analysis are shown in Fig.4. Then, the deflection angle of front rotor is kept constant as θ_f=-4[deg], where the maximum efficiency is obtained. Each axes and calculation method are the same as Fig.3. As a careful point, each parameters of rear rotor P_r, H_r and η_r correspond to each parameters of front rotor P_f, H_f and η_f respectively. Therefore, the total pressure efficiency of rear rotor η_r was expressed in the following equation.

$$\eta_r = \frac{P_r}{\rho g Q H_r}$$

In the rear rotor shown in Fig.4, the turbine head H_r and shaft power P_r increased according to the increase of deflection angle. The maximum efficiency $\eta_{r\,max}$=66.9[%] was obtained at θ_r=10[deg]. The efficiency was approximately constant until θ_r=10[deg], and decreased after θ_r=10[deg], according to the increase of deflection angle.

And, the total pressure efficiency of this hydroturbine η was expressed in the following equation.

$$\eta = \frac{P_f + P_r}{\rho g Q H}$$

This hydroturbine head H was obtained from inlet interface of front rotor and outlet interface of rear rotor. When both front and rear rotors were the maximum efficiency, total efficiency η=60.5[%] was obtained.

When the deflection angle was changed, the total pressure efficiency variation of the front rotor was bigger than that of the rear rotor. The relationship between the performance and internal flow was investigated by the numerical analysis results at the deflection angle of each maximum and minimum efficiencies.

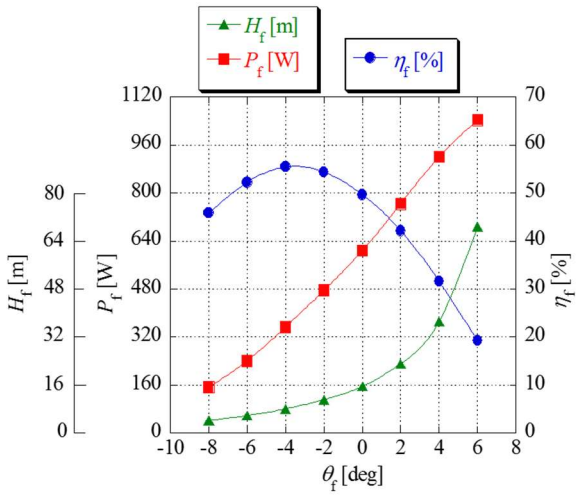

Fig.3 Performance curves of front rotor by the deflection angle (Q=1.0Q_d)

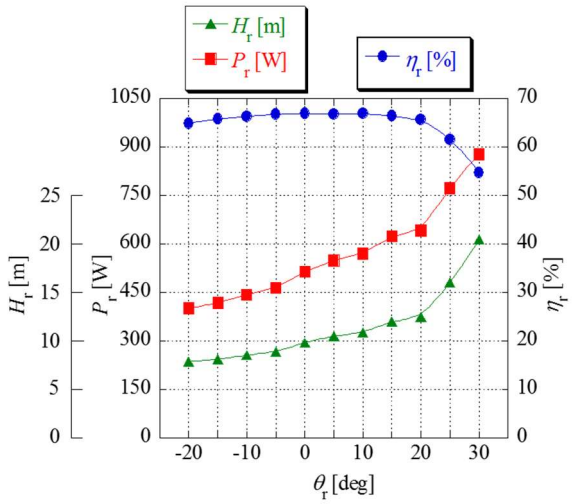

Fig.4 Performance curves of rear rotor by the deflection angle (Q=1.0Q_d)

4.2. Internal flow of each deflection angle

Relative velocity vectors around the blade of front rotor are shown in Fig.5. The position is blade width center (B/B_c=0.5). B is a blade width position and B_c is a width between hub and the casing. The rotational direction of the front rotor is the upper side of the paper. Left side of the paper is inlet side of front rotor, and right side of the paper is outlet side of front rotor. The flow rate is the design flow rate 1.0Q_d. The deflection angle of front rotor θ_f=-8[deg] is the minimum efficiency in small deflection angle, θ_f=-4[deg] is the maximum efficiency, θ_f=6[deg] is the minimum efficiency in large deflection angle. In all of them, these fluids were flowing along the blade, and there was no separation of flow. The same tendency could be confirmed also at the hub side and the tip side. Therefore, the cause of efficiency decline isn't separation of flow according to the variation of deflection angle. The relative velocity distributions around the blade of front rotor are shown in Fig.6. The conditions are the same as Fig.5. The relative velocity at θ_f=6[deg] was largest at outlet side of the front rotor. When the deflection angle was made large, the outlet angle of front rotor became small because the inlet angle

was constant. In this case, the inlet flow condition was assumed to be uniform. As the result, blade-to-blade passage near the outlet of front rotor became narrow, and the velocity increased as could be confirmed in Fig.6(c). Therefore, there was no separation in the front rotor, but the friction loss was increased, and the efficiency of front rotor was decreased. On the other hand, the relative velocity at θ_f=-8[deg] was decreased at the around middle of inlet and outlet of the front rotor. The static pressure distributions around the blade of front rotor are shown in Fig.7. The conditions are the same as Fig.5 and Fig.6. In θ_f=-8[deg], adverse pressure gradient occurred in blade-to-blade passage. When the deflection angle was made small, the outlet angle of front rotor became large because the inlet angle was constant. As the result, the turbine head was made small and blade-to-blade passage of front rotor became wide. Therefore, it was easy to decrease the relative velocity and to bring about adverse pressure gradient, so it was considered that the efficiency of front rotor was decreased by deceleration loss.

Next, relative velocity vectors around the blade of rear rotor are shown in Fig.8. The position is blade width center (B/B_c=0.5). The rotational direction of the rear rotor is the down side of the paper. Left side of the paper is inlet side of rear rotor, and right side of the paper is outlet side of rear rotor. The flow rate is the design flow rate 1.0Q_d. The deflection angle of rear rotor θ_r=10[deg] is the maximum efficiency, θ_r=30[deg] is the minimum efficiency. Then, the deflection angle of front rotor is kept constant as θ_f=-4[deg], where the maximum efficiency is obtained. In both θ_r=10[deg] and θ_r=30[deg], these fluids were flowing along the blade, and there was no separation of flow. The same tendency could be confirmed also at the hub side and the tip side. The relative velocity distributions around the blade of rear rotor are shown in Fig.9. The conditions are the same as Fig.8. The relative velocity at θ_r=30[deg] was larger than that at θ_r=10[deg] at outlet side of rear rotor. As with front rotor, when the deflection angle was made large, the blade-to-blade passage near the outlet of rear rotor became narrow, the velocity increased as shown in Fig.9(b). Therefore, the friction loss was increased, and the efficiency of rear rotor was decreased as the same with the front rotor when the deflection angle of the rear rotor increased.

When the front and rear rotors are compared, the relative velocity in the outlet side of front rotor is larger than that of the rear rotor, and the flow passage length of the front rotor from the inlet to outlet is long. Therefore, the loss of front rotor is big, and we consider that the efficiency of front rotor becomes lower than that of the rear rotor.

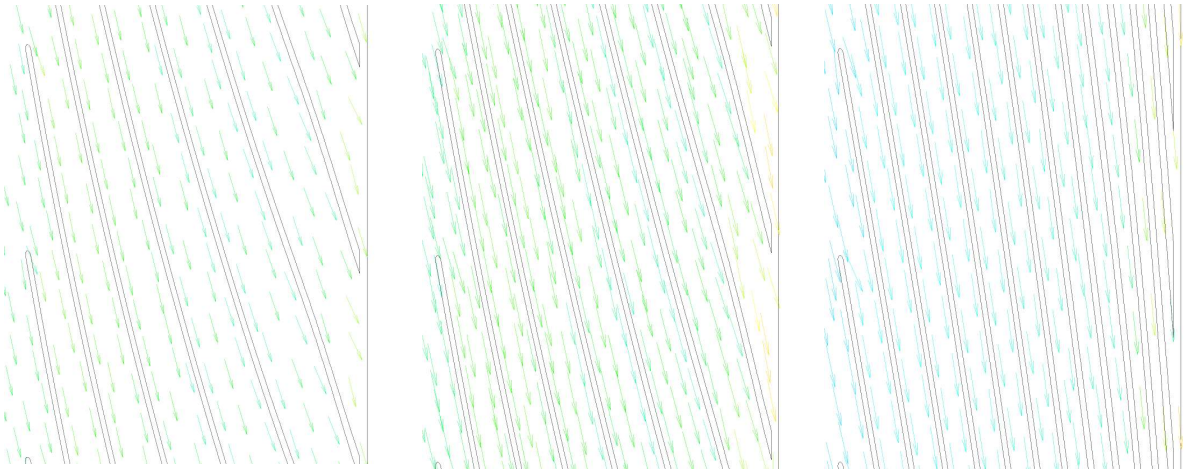

(a) θ_f=-8[deg] (b) θ_f=-4[deg] (c) θ_f=6[deg]

Fig.5 Relative velocity vectors of front rotor (Q=1.0Q_d, B/B_c=0.5)

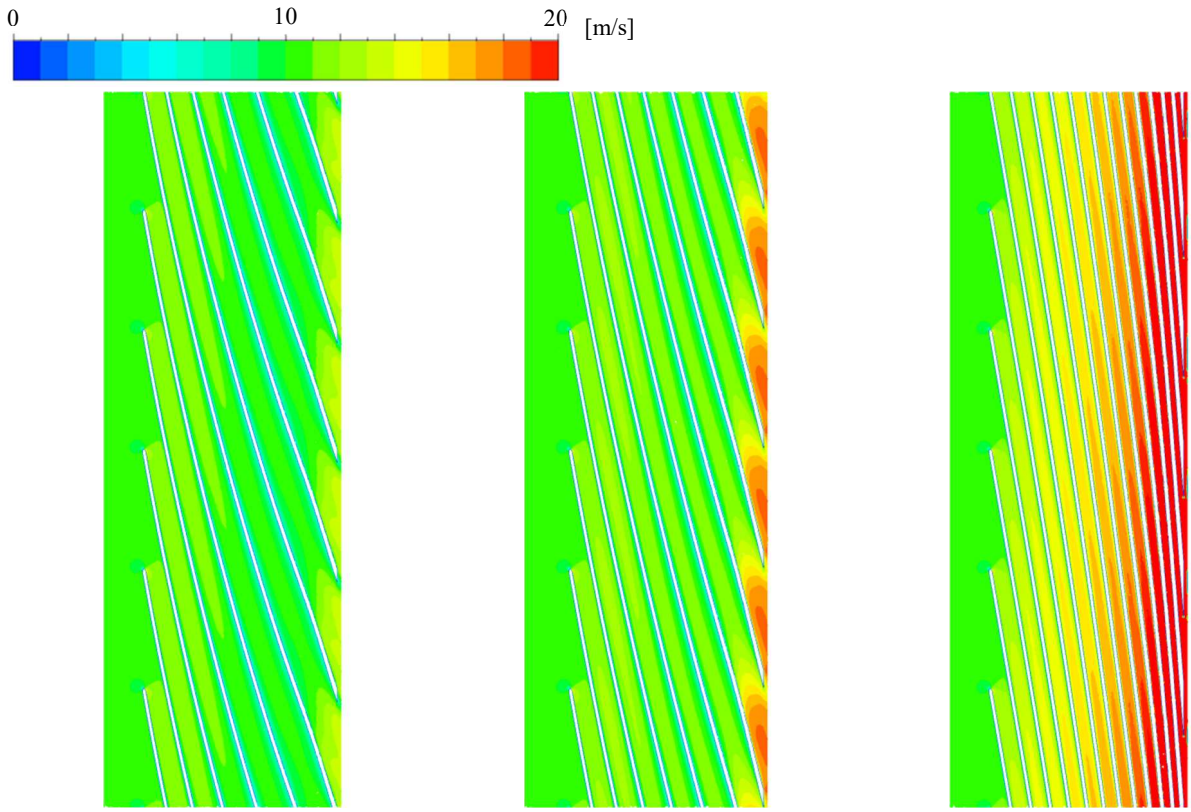

(a) θ_f=-8[deg] (b) θ_f=-4[deg] (c) θ_f=6[deg]

Fig.6 Relative velocity contour maps of front rotor (Q=1.0Q_d, B/B_c=0.5)

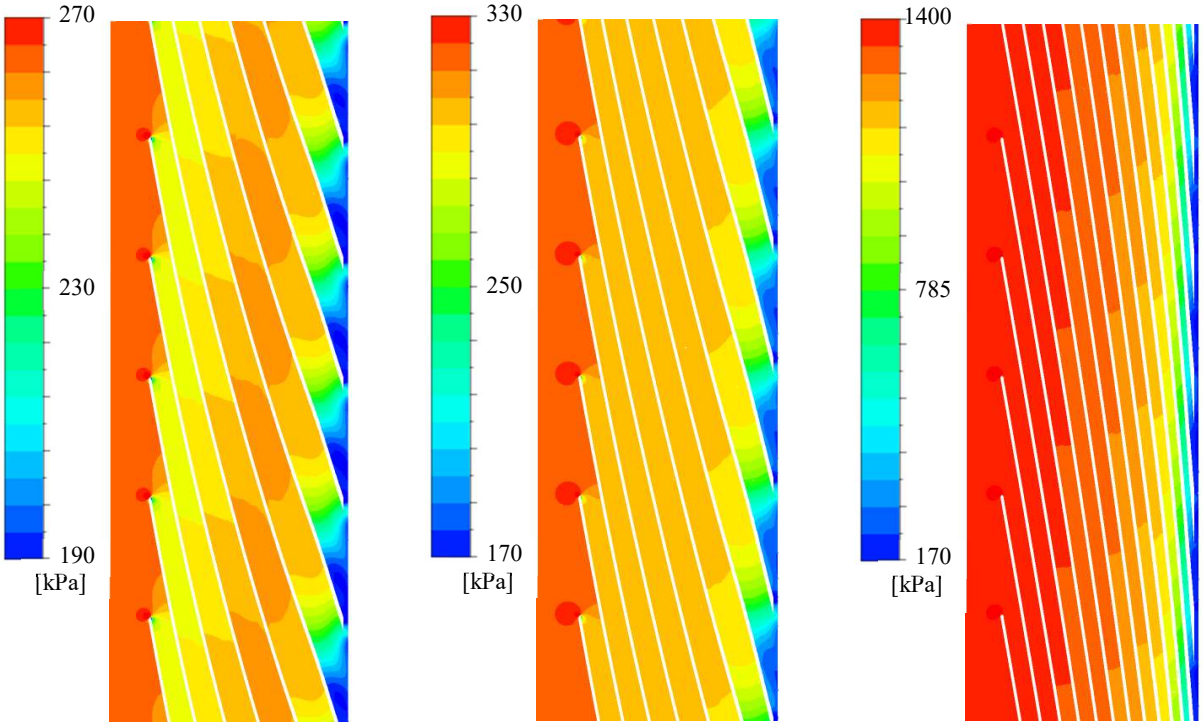

(a) θ_f=-8[deg] (b) θ_f=-4[deg] (c) θ_f=6[deg]

Fig.7 Static pressure contour maps of front rotor (Q=1.0Q_d, B/B_c=0.5)

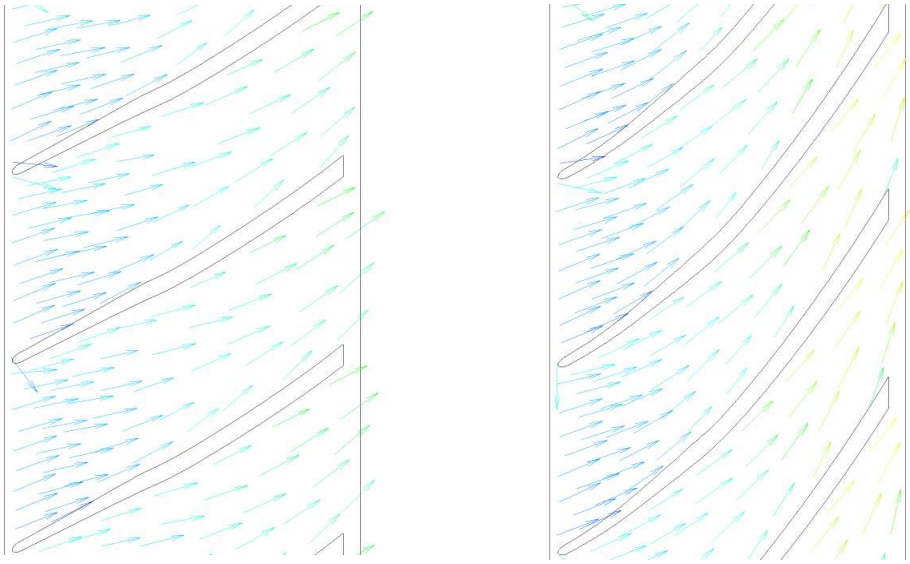

(a) θ_r=10[deg] (b) θ_r=30[deg]

Fig.8 Relative velocity vectors of rear rotor (Q=1.0Q_d, B/B_c=0.5)

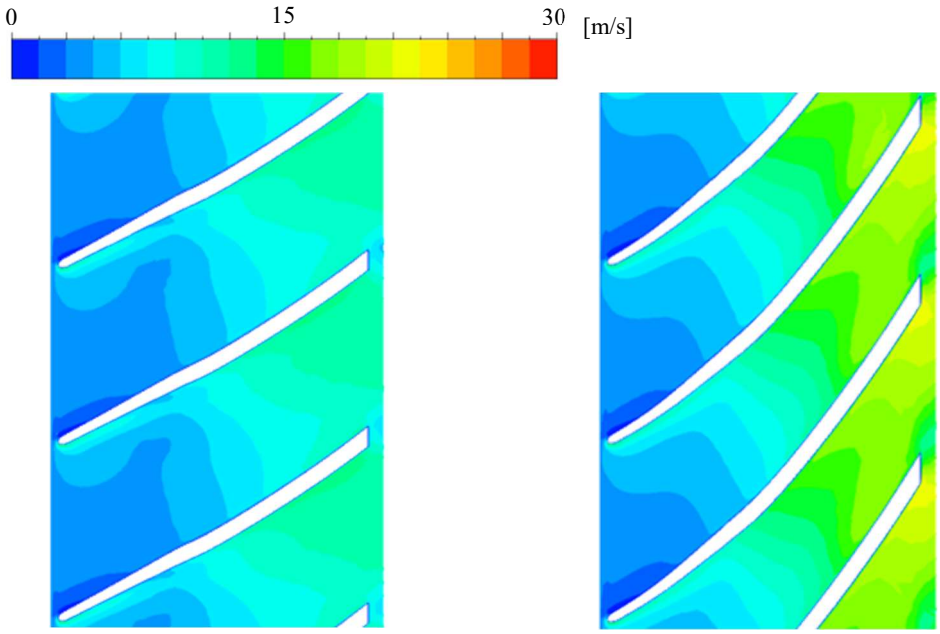

(a) θ_r=10[deg] (b) θ_r=30[deg]

Fig.9 Relative velocity contour maps of rear rotor (Q=1.0Q_d, B/B_c=0.5)

5. Concluding remarks

The influence of deflection angle on the performance of the new contra-rotating small hydroturbine composed of the hybrid rotor and centrifugal rotor were investigated by the numerical analysis results. As a result, the following conclusions were obtained.

(1) In this new type hydroturbine, the maximum efficiency of the front rotor $\eta_{f\,max}$=55.5[%] was obtained at θ_f=-4[deg], and that of the rear rotor $\eta_{r\,max}$=66.9[%] was obtained at θ_r=10[deg].

(2) When the deflection angle of this hydroturbine was made big, the blade-to-blade passage of rotor became narrow near the outlet of rotor, and the relative velocity was increased at outlet side of each front and rear rotors. Therefore, there was no separation of flow in rotor, but the friction loss was increased near the outlet of rotor. As the result, the efficiency was decreased.

(3) In the front rotor of this hydroturbine, when the deflection angle was made small, the turbine head was made small and blade-to-blade passage of front rotor became wide. Therefore, it was easy to decrease the relative velocity and to bring about adverse pressure gradient, as the result, the efficiency of front rotor was decreased by deceleration loss.

(4) The relative velocity in outlet side of front rotor was bigger than that of the rear rotor, and the flow passage lenght of the front rotor from inlet to outlet was long. Therefore, the loss of front rotor was made bigger, and the influence of deflection angle of the front rotor was bigger than the rear rotor.

References

[1] Furukawa A, Okuma K and Tagaki A 1998 Basic study of low head water power utilization by using darrieus-type turbine *Trans. JSME (in Japanese)* **64** 2534-40

[2] Kanemoto T, Inagaki A, Misumi H and Kinoshita H 2004 Development of gyro-type hydraulic turbine suitable for shallow stream (1st report, Rotor works and hydroelectric power generation) *Trans. JSME (in Japanese)* **70** 413-8

[3] Matsui J 2010 Internal flow and performance of the spiral water turbine *Turbomachinery (in Japanese)* **38** 358-64

[4] Ikeda T, Iio S and Tatsuno K 2010 Performance of nano-hydraulic turbine utilizing waterfalls *Renewable Energy* **35** 293-300

[5] Nakajima M, Iio S and Ikeda T 2008 Performance of savonius rotor for environmentally friendly hydraulic turbine *Journal of Fluid Science and Technology* **3** 420-9

[6] Iio S, Uchiyama F, Sonoda C and Ikeda T 2009 Performance improvement of savonius hydraulic turbine by using a shield plate *Turbomachinery (in Japanese)* **37** 743-8

[7] Shigemitsu T, Fukutomi J and Tanaka C 2015 Challenge to use small hydro power by contra-rotating small hydro-turbine *Renewable Energy in the Service of Mankind* **1** 317-27

[8] Sonohata R, Fukutomi J and Shigemitsu T 2012 Study on the contra-rotating small-sized axial flow hydro turbine *Open Journal of Fluid Dynamics* **2** 318-23

[9] Shigemitsu T, Fukutomi J and Sonohata R 2013 Performance and internal flow of contra-rotating small hydro turbine *Proc. Int. Conf. ASME 2013 Fluids Engineering Division Summer Meeting* FEDSM2013-16274

[10] Shigemitsu T, Fukutomi J and Tanaka C 2013 Unsteady flow condition of contra-rotating small-sized hydro turbine *Proc. the 12th Asian Int. Conf. on Fluid Machinery* AICFM12-0019

[11] Shigemitsu T, Takeshima Y, Tanaka C and Fukutomi J 2015 Influence of spoke geometry on performance and internal flow of contra-rotating small-sized hydroturbine *Proc. the ASME/JSME/KSME 2015 Joint Fluids Engineering Conf.* AJK2015-22116

[12] Shigemitsu T, Takeshima Y, Ogawa Y, Ding N and Fukutomi J 2016 Pressure fluctuation near blade of contra-rotating small hydroturbine *Turbomachinery (in Japanese)* **44** 41-9